NACA RM A52D01b

NACA

RESEARCH MEMORANDUM

BOUNDARY-LAYER MEASUREMENTS ON SEVERAL POROUS MATERIALS WITH SUCTION APPLIED

By George B. McCullough and Bruno J. Gambucci

Ames Aeronautical Laboratory
Moffett Field, Calif.

NATIONAL ADVISORY COMMITTEE
FOR AERONAUTICS

WASHINGTON
June 18, 1952

NATIONAL ADVISORY COMMITTEE FOR AERONAUTICS

RESEARCH MEMORANDUM

BOUNDARY-LAYER MEASUREMENTS ON SEVERAL POROUS MATERIALS WITH SUCTION APPLIED

By George B. McCullough and Bruno J. Gambucci

SUMMARY

Boundary-layer velocity profiles were measured on ten samples of various porous materials and on an impervious aluminum plate mounted flush with the inner surface of the side wall of a small wind tunnel. Suction was applied to the back side of the porous test materials through a 4-inch-square opening. The profiles were measured after the natural boundary layer of the tunnel wall had traversed a distance of 3-1/2 inches along the suction area.

The boundary layer measured on the smooth impervious plate was laminar at the upstream end of the suction area, but was of the transitional type after having traversed the 3-1/2 inches to the downstream measuring station. Without suction none of the velocity profiles measured on the porous materials were laminar at the downstream station. The thickness of the boundary layer was increased and its form altered from that measured on the impervious plate by amounts which depended on the nature of the surface of the material. With suction applied the form of the boundary layers was greatly altered, and both the displacement thickness and the momentum thickness were reduced. The rate of thinning diminished with increasing suction, and the boundary-layer displacement and momentum thicknesses on all of the porous materials appeared to be approaching a low ultimate value with increasing suction velocity.

INTRODUCTION

A method of boundary-layer control based on the continuous removal of a portion of the boundary-layer flow along a porous surface has been the subject of several recent investigations. This method has been termed "distributed" or "area suction" to distinguish it from suction through discrete slots cut in an otherwise impervious surface, and has received particular attention because theoretical analyses indicate that

it is more economical of power than the method employing slots. Area suction may be used for three general purposes: to increase the maximum lift of a wing by delaying separation of either the laminar boundary layer near the leading edge or the turbulent boundary layer near the trailing edge; to reduce drag by delaying transition of the boundary-layer flow to turbulence; or to improve the efficiency of inlets or diffusers by thinning the boundary-layer flow (references 1, 2, and 3).

The investigation reported herein was made in connection with an investigation of area suction intended to delay separation of the laminar boundary layer near the leading edge of an airfoil section. It was the the purpose of the present investigation to gain in a quick and simple manner some idea of the importance of the nature of the surface of various porous materials on the boundary layer flowing over the materials. Precise and detailed measurements which would provide a check on the theory of boundary-layer flow with porous suction were not made, nor were measurements made of the pressure differential or power required to induce the suction flow. It was felt, however, that the information obtained would serve as a rough guide for the selection of porous materials where it was desired to maintain the thinnest possible boundary layer with the minimum volume of suction flow.

The tests were made in a small wind tunnel and consisted of measurements of the boundary-layer velocity profiles on small samples of various porous materials inset into the side walls of the wind tunnel. Measurements were made for several ratios of the average suction velocity to free-stream velocity from 0 to 0.0182. In addition, measurements were made on a smooth, impervious aluminum plate to serve as a basis for assessing the effects of the roughness of the porous materials.

NOTATION

A	nominal area to which suction was applied, 0.111 square feet
g	acceleration of gravity, 32.2 feet per second squared
h	local total pressure within boundary layer, pounds per square foot
H	settling-chamber total pressure, pounds per square foot
p_o	reference static pressure measured at entrance to test section, pounds per square foot
p	local static pressure measured along center line of test-section wall, pounds per square foot

u local velocity within boundary layer $\left(\sqrt{\frac{2}{\rho_o}(h-p)}\right)$, feet per second

U_1 local velocity outside of boundary layer, feet per second

U_o free-stream velocity $\left(\sqrt{\frac{2}{\rho_o}(H-p_o)}\right)$, feet per second

v_s average suction velocity $\left(\frac{W_a}{g\rho_o A}\right)$, feet per second

y distance from surface, inches

R_{δ^*} boundary-layer Reynolds number $\left(\frac{U_1\delta^*}{\nu}\right)$

R_θ boundary-layer Reynolds number $\left(\frac{U_1\theta}{\nu}\right)$

W_a weight rate of suction flow, pounds per second

δ boundary-layer thickness, inches

δ^* boundary-layer displacement thickness $\left[\int_o^\delta \left(1-\frac{u}{U_1}\right)dy\right]$, inches

θ boundary-layer momentum thickness $\left[\int_o^\delta \frac{u}{U_1}\left(1-\frac{u}{U_1}\right)dy\right]$, inches

ν kinematic viscosity, feet squared per second

ρ_o free-stream density, slugs per cubic foot

[redacted]

MATERIALS AND APPARATUS

Materials

Ten samples of four different types of porous materials were investigated. All of the materials are commercially available as flat sheets. The samples were 4-5/8 inches square, and the thickest one did not exceed 3/32 inch. The various samples are listed in table I together with remarks about the surface roughness. Photographs of the samples, both direct and with a magnification factor of 21, are presented in figure 1.

One of the materials was a laboratory-type filter paper which required additional support in the wind tunnel, and hence was tested with two different backing materials: a 16 mesh, 0.023-inch-diameter wire screen (sample 1), and a flat, electroplated, 40-count metal mesh (sample 2).

The second type of material was a woven wire filter cloth with 250 woof (longitudinal) threads and 20 warp (transverse) threads per inch. This material was tested in two positions; that is, with the woof parallel with the flow (sample 3), and with the warp parallel with the flow (sample 4).

The third type of material was a metal mesh with square openings made by an electroplating process. Two sizes of mesh, 40 count (sample 5), and 65 count (sample 6), were tested. The percent open area of the 40-count mesh was 23.0, and of the 65-count mesh was 10.5.

The fourth type of material was sintered bronze of which four samples of varying porosity were tested. Samples 7, 8, and 9 were intended for use in filters, and sample 10 was originally impregnated with oil for use in bearings. The oil was removed for these tests, but the porosity was so low that only low suction velocities could be attained with the suction pump.

The degree of surface roughness varied greatly between the various samples. Because of the nature of the materials it is difficult to assess the surface roughness from purely geometric considerations. This is particularly true of the wire cloth and the electroplated mesh. Also the surfaces of the samples of sintered bronze are not analogous to the surface of a smooth flat plate on which small granules of some sandlike material have been sprinkled in such a manner that each grain can be considered as an individual roughness element. Measurements were made, however, with the aid of an instrument which drew greatly magnified profiles of the surface of the filter paper and the sintered bronzes. These profiles were difficult to interpret in terms of roughness because the

datum or "surface" from which the height of the roughness elements were to be measured was not clear. Instead, the average total amplitude of each set of curves was taken as a measure of the surface roughness. The sintered bearing material (sample 10) felt as smooth to the touch as the aluminum plate on which the basic boundary-layer velocity profiles were obtained. All the other samples felt rougher in varying degrees.

Wind Tunnel

The small wind tunnel used in the investigation is of the nonreturn type and has a closed, rectangular throat. The tunnel is powered by a variable-speed electric motor which drives an aircraft-type centrifugal compressor (supercharger). The air is pumped into a settling chamber where it passes through four fine-mesh wire screens before entering the contraction cone. From the contraction cone the air flows through a rectangular test section and is exhausted to the atmosphere through a diffuser. The dimensions of the throat are 2.1 by 7.4 inches. The floor and ceiling (2.1-inch dimension) of the test section diverge a total of 1.0° in the vertical plane to compensate partially for boundary-layer growth. The contraction ratio of the tunnel is 15.5 to 1. The turbulence level is unknown.

Auxiliary Equipment

The 4-5/8-inch-square test samples were mounted in a recess over a 4-inch-square opening symmetrical with the center line of the test-section side wall. The porous materials, therefore, overlapped the suction area by 5/16 inch on all four sides. The upstream edge of the suction area was 3/8 inch downstream of the beginning of the test section. A photograph of a test sample mounted in the wind tunnel is shown in figure 2.

A plenum chamber was fastened to the outside of the tunnel wall and was connected by a duct containing an orfice-type flow meter to an annular ejector pump. This pump was operated by compressed air, the flow of which was manually regulated to produce the desired suction velocity through the porous material. The ejector pump exhausted into the diffuser of the wind tunnel. A diagram of the arrangement is shown in figure 3.

The boundary-layer velocity profiles were measured with a single total-pressure tube. The shank of the tube was bent at right angles and projected through a tight-fitting hole in the side of the tunnel. The height of the tube above the surface could thus be changed from outside

the tunnel. The distance of the tube above the surface was read on an Ames dial gage. The surface was defined as the level indicated by the dial gage with the tip of the probe just touching the porous surface. In some cases the point of first contact was verified with the tunnel running by measuring the electrical resistance between the probe and the porous metal. The tip section of the probe was made of 0.015-inch-diameter, 0.0025-inch-wall-thickness tubing flattened to 0.010 inch. The geometric center of the tube was taken as the effective center. The distance above the surface corresponding to each determination of the local velocity within the boundary layer, therefore, was taken as the net reading of the dial gage plus 0.005 inch. In most cases the effective or aerodynamic surface of the porous material was undoubtedly below the nominal surface by an amount which depended on the heights of the roughness elements, but because of the previously mentioned uncertainty in the measurements of surface roughness, no corrections were applied to take this factor into account. The axis of the probe was in the median plane of the tunnel with the tip extending 1/2 inch ahead of the downstream edge of the suction area. The boundary layer on the tunnel wall traveled a distance of 3-1/2 inches over the suction area before reaching the measurement station. With the aluminum plate installed in the tunnel, an additional measurement was made at the upstream boundary of the suction area. With the porous materials the presence of the plenum chamber on the outside of the test-section wall made it impractical to install the probe at this upstream station.

TESTS AND RESULTS

Each test sample was carefully fitted into the test-section wall and, except for the samples of filter paper, the joints and screw holes were filled with surfacing putty which was sanded down flush with the surface. The filter paper was faired in with modeling clay to avoid the sanding operation.

The dynamic pressure was held constant at 30 pounds per square foot which corresponds to a tunnel speed of about 165 feet per second and a Mach number of 0.143. The Reynolds number per foot of length was about 1,000,000. For the porous materials, five rates of the average suction velocity were used: 0, 0.6, 1.0, 2.0, and 3.0 feet per second.

The distribution of static pressure along the center line of the side wall of the wind tunnel is shown in figure 4. The boundary-layer velocity profiles measured on the aluminum plate are shown in figure 5. The two profiles shown for the downstream station were measured for two different installations of the plate. Because repeat runs for the same installation showed good agreement, the difference in the two profiles can be attributed only to differences in the degree of smoothness of the

[redacted]

joints in the test-section wall. The boundary-layer profiles measured on the porous materials are shown in figure 6. It is possible that these measurements were also affected by the degree of smoothness with which the various samples were fitted into the wall, but any discrepancies in the data from this cause would not be sufficient to alter the general conclusions of this report. Also shown for comparison is the thicker of the two velocity profiles measured at the same station on the aluminum plate.

DISCUSSION

Measurements on the Impervious Plate

In considering the boundary-layer measurements on the impervious plate, there are several factors to be noted which would influence the growth of the boundary layer up to the plate. The boundary-layer flow prior to reaching the test region was subjected to acceleration in the contracting section of the tunnel. The boundary-layer measurements, however, were made in a region of essentially zero pressure gradient (fig. 4). Also, although pains were taken to keep the tunnel wall smooth, the flow may have been subjected to two surface discontinuities, one at the upstream edge of the removable side wall and the other at the upstream edge of the inset test plate.

The velocity profile measured at the upstream end of the plate (fig. 5) was of the laminar type and showed the effect of the acceleration in the contracting section of the tunnel. It was typical of the laminar type in a favorable pressure gradient as shown by comparison with a profile computed by the Pohlhausen approximate method for $\lambda = +12$. (The parameter λ specifies the velocity gradient, and +12 corresponds to the most favorable gradient the method will permit without producing unrealistic profiles. See reference 4.)

At the downstream station a difference in velocity profile was obtained, as previously mentioned, for two different installations of the test plate which was apparently due to differences in the surface condition at the upstream end of the test plate. The two profiles resembled neither laminar nor fully developed turbulent profiles. It is probable that the measurement station was in a region of intermittent transition and, therefore, the measured velocity profiles represent the time average of fluctuating dynamic pressures within the boundary layer.

In an attempt to shed further light on the nature of the boundary layers, the boundary-layer Reynolds number R_θ and R_{δ^*} were computed using values of the momentum thickness θ and the displacement thickness δ^* obtained by mechanical integration of the velocity profiles.

[redacted]

At the upstream station the respective values were: θ, 0.0045 inch; δ^*, 0.0091 inch; R_θ, 367, and R_{δ^*}, 745. While the value of R_{δ^*} is not high for a laminar boundary layer in a zero pressure gradient, it is sufficiently large to indicate that transition could be imminent in a stream with a moderately high level of turbulence. At the downstream station, the thicker of the two profiles gave the following values: θ, 0.0117 inch; δ^*, 0.0186 inch; R_θ, 956, and R_{δ^*}, 1520. Although the magnitude of R_{δ^*} is not beyond the realm of possiblity for a laminar boundary layer, the shape of the velocity profile indicates that it is not laminar. If the boundary layer is undergoing transition, as is believed to be the case, then the computed values of the boundary-layer parameters have little meaning because they do not represent a steady-state velocity profile.

Measurements on Porous Materials Without Suction

For zero suction velocity, the porous sample which produced the least effect on the boundary layer was sample 10 (the bearing material). The velocity profile was almost identical with that on the aluminum plate (fig. 6(j)). It was, however, the most dense of all the porous samples and permitted a maximum suction velocity of only 1.0 foot per second with the suction pump used.

Aside from sample 10, the two smoothest samples were the filter paper, which showed little effect of the types of backing (figs. 6(a) and (b)), and the sintered bronze, sample 9 (fig. 6(i)). The velocity profiles for zero suction on both of these materials showed a considerable difference from the velocity profile on the aluminum plate, and are definitely of the turbulent type.

The profiles measured with samples 3 to 8 (figs. 6(c) to 6(h)) showed large effects of surface roughness. The profile which showed the greatest difference from that measured on the aluminum plate was that for sample 5, the coarser of the two electroplated meshes. The orientation of the wire cloth (figs. 6(c) and 6(d)) also had an effect on the boundary layer: a thicker profile resulted with the warp parallel to the flow than with the woof parallel to the flow.

Measurements on Porous Materials With Suction

The effect of suction on the boundary-layer velocity profiles on all of the porous materials was about the same. The velocity near the surface was increased, and the total thickness of the boundary layer was reduced. In order to illustrate further the effect of suction, each velocity profile was integrated and the boundary-layer displacement

thickness δ^*, and the momentum thickness θ ascertained. The values of these parameters are plotted in figure 7 as functions of the suction velocity ratio v_s/U_o. The trend is the same for all materials; a rapid decrease of δ^* and θ with increasing suction velocity ratio. Both δ^* and θ appear to be approaching small ultimate values for high suction velocity ratios. From considerations of attaining the thinnest possible boundary layer with the minimum suction velocity, materials which are physically smooth with small closely spaced pores such as samples 8, 9, or 10 are best. Materials with definite open spaces like the electroplated meshes are poor. For high suction-velocity ratios, however, the degree of surface roughness appears to be of diminishing importance as compared to the case for zero suction. If the power required to produce the suction is taken into consideration, the choice of materials may be considerably affected because a large power requirement may more than counterbalance the apparent advantage offered by a dense smooth-surfaced material.

In an attempt to shed further light on the nature of the profiles measured with suction in the present investigation, comparison was made with the profiles presented in references 3 and 5. These references report the results of boundary-layer measurements made on a flat, porous plate with suction, and compare the experimentally derived profiles with those predicted by theory. Reference 3 is concerned with turbulent flow and reference 5 with laminar flow. Neither the theoretical nor the experimental laminar suction profiles of reference 5 (which were in good agreement) are similar to the suction profiles of the present investigation; hence it may be concluded that the latter are not laminar. They are, however, similar to the turbulent suction profiles of reference 5. It is also shown in reference 5 that an asymptotic turbulent profile, analogous to the asymptotic laminar profile, can be attained with turbulent flow (i.e., that there will be no further change in the boundary-layer profile with increasing distance downstream). A method for computing the shape of the asymptotic turbulent profile is derived and, according to this analysis, the portion of the profile outside the laminar sublayer is a function of the logarithm of the distance from the surface. A simple check on experimental profiles can be obtained by plotting the values of $\left(1 - \frac{u}{U_o}\right)$ against $\log_e y$. For an asymptotic turbulent profile the outer portion of the boundary layer should be a straight line. The suction profiles measured in the present investigation were plotted in this manner and did not produce straight lines even though the suction-velocity ratios were higher than those employed in reference 3. This would indicate that the length of the suction area in the present investigation (3-1/2 in.) was not sufficient for the velocity profile to attain its ultimate form.

[redacted]

CONCLUDING REMARKS

From the measurements of boundary-layer velocity profiles on several porous materials for ratios of suction velocity to free-stream velocity varying from 0 to 0.0182, it was shown that for zero and low values of suction velocity the degree of surface roughness produced a considerable effect on the thickness of the boundary layer; the greater the surface roughness, the thicker the boundary layer. Materials such as the flat metal meshes with definite open spaces, although smooth to the touch, were shown to be aerodynamically rough. In general, increasing the suction velocity reduced the boundary-layer thickness rapidly at first; then, at a rate which diminished with increasing suction. The boundary-layer displacement thickness and momentum thickness for all the porous materials appeared to be approaching a low ultimate value for suction-velocity ratios greater than the maximum attained in these tests.

Ames Aeronautical Laboratory
National Advisory Committee for Aeronautics
Moffett Field, Calif.

REFERENCES

1. Thwaites, B.: A Theoretical Discussion of High-Lift Aerofoils with Leading-Edge Porous Suction. R. & M. No. 2242, British A.R.C., 1946.

2. Ulrich, A.: Theoretical Investigation of Drag Reduction in Maintaining the Laminar Boundary Layer by Suction. NACA TM 1121, 1947.

3. Kay, J. M.: Turbulent Boundary Layer Flow with Uniform Suction. British A.R.C. 12,193, 1949.

4. Durand, W. F., ed., Aerodynamic Theory. Vol. III, Julius Springer (Berlin), 1934.

5. Kay, J. M.: Experimental Investigation of Boundary Layer Flow Along a Flat Plate with Uniform Suction. British A.R.C. 11,476, 1948.

TABLE I.- LISTING OF THE SAMPLES TESTED

Sample number	Figure number of photograph	Type of material	Remarks	Measured roughness (in.)
1	1(a)	Filter paper	Backed with wire screen	[a]0.0007
2	1(a)	- - do. - -	Backed with electroplated mesh	[a]0.0007
3	1(b)	Woven wire cloth	Woof parallel with flow	- - -
4	1(b)	- - do. - -	Warp parallel with flow	- - -
5	1(c)	Square mesh made by electroplating	40 count	- - -
6	1(d)	- - do. - -	65 count	- - -
7	1(e)	Sintered bronze	Manufacturers' grade 2	[b]- - -
8	1(f)	- - do. - -	Manufacturers' grade 4	0.005
9	1(g)	- - do. - -	- - - -	0.0025
10	1(h)	- - do. - -	De-oiled bearing material	0.0012

[a]This low measured value is probably misleading because the softness of the paper may have allowed surface fibers to sink into the body of the paper under the pressure of the measuring stylus.

[b]Too rough to measure directly, but average diameter of individual particles appeared to be at least ten times greater than that of grade 4.

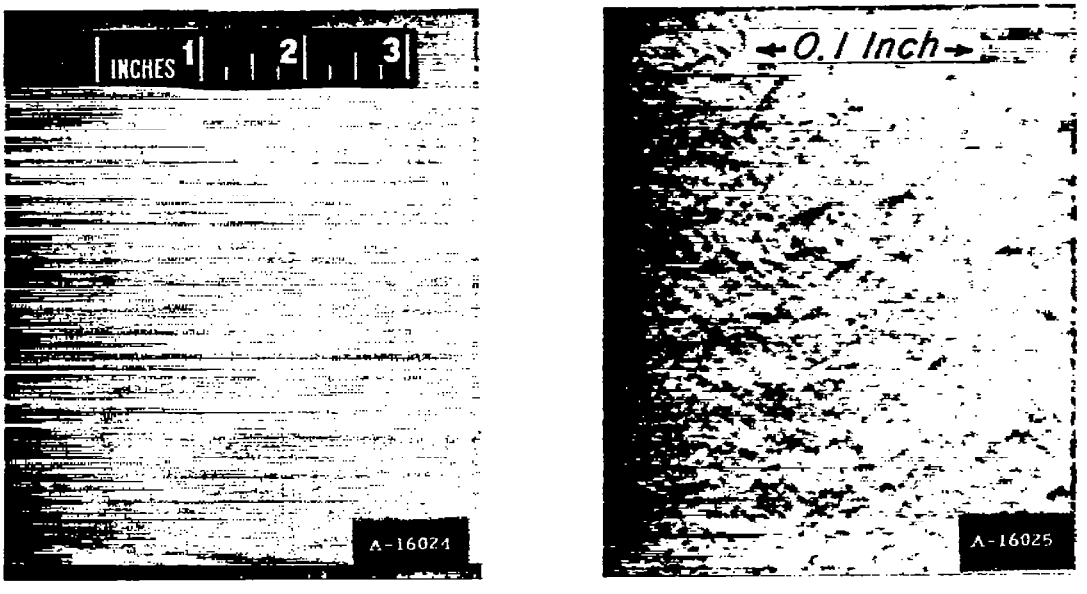

(a) Samples 1 and 2 (filter paper).

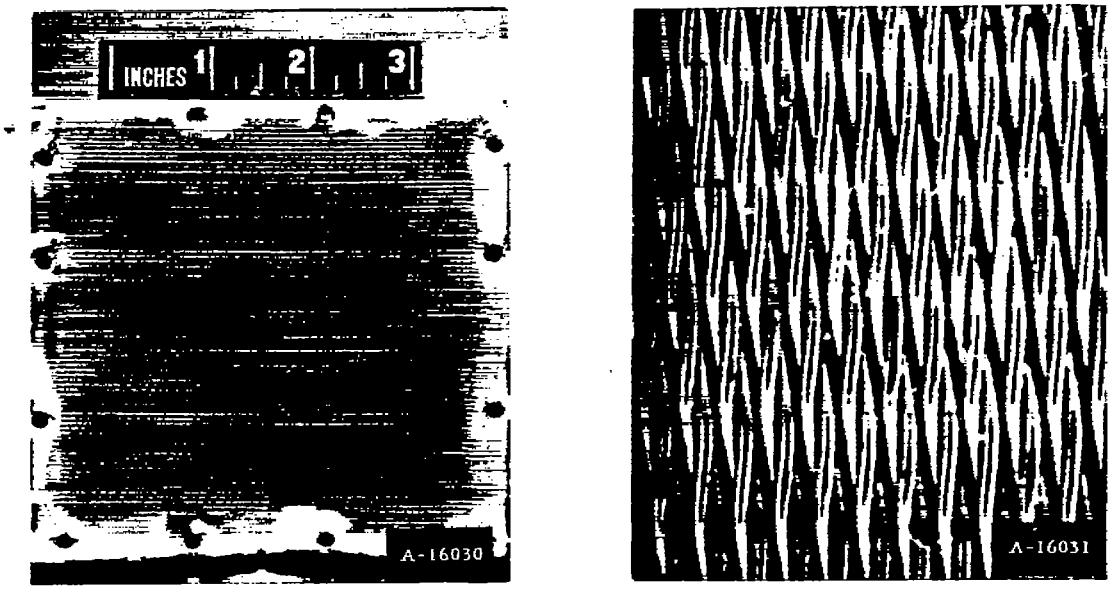

(b) Samples 3 and 4 (wire cloth).

Figure 1.- Photographs of the samples of porous materials. Magnification ratio is 21X.

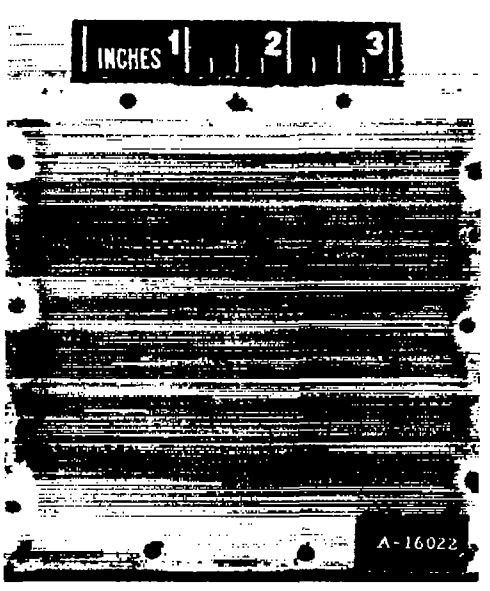

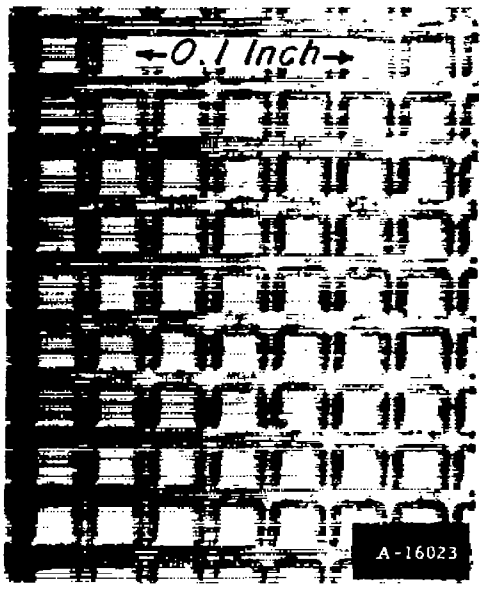

(c) Sample 5 (40-count mesh).

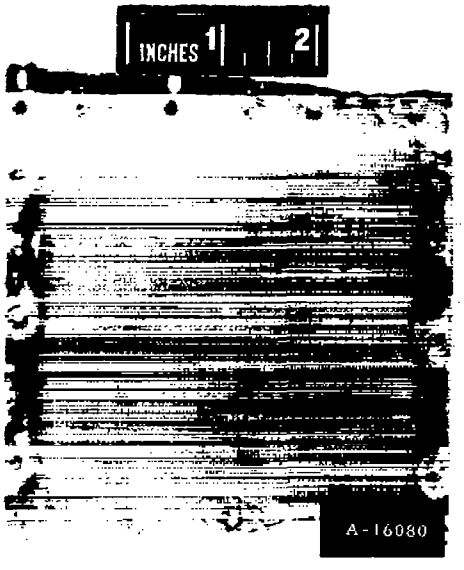

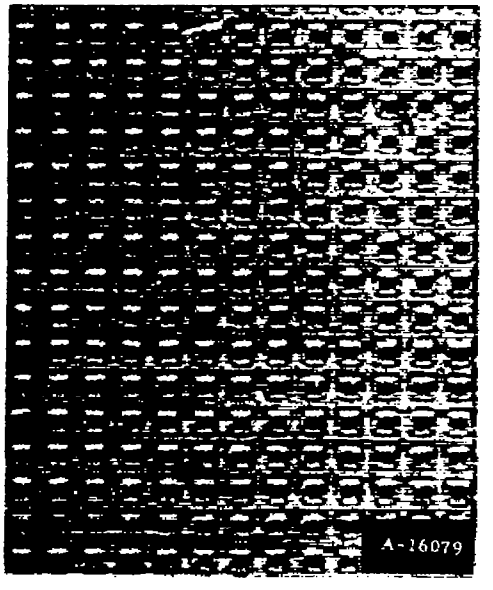

(d) Sample 6 (65-count mesh).

Figure 1.- Continued.

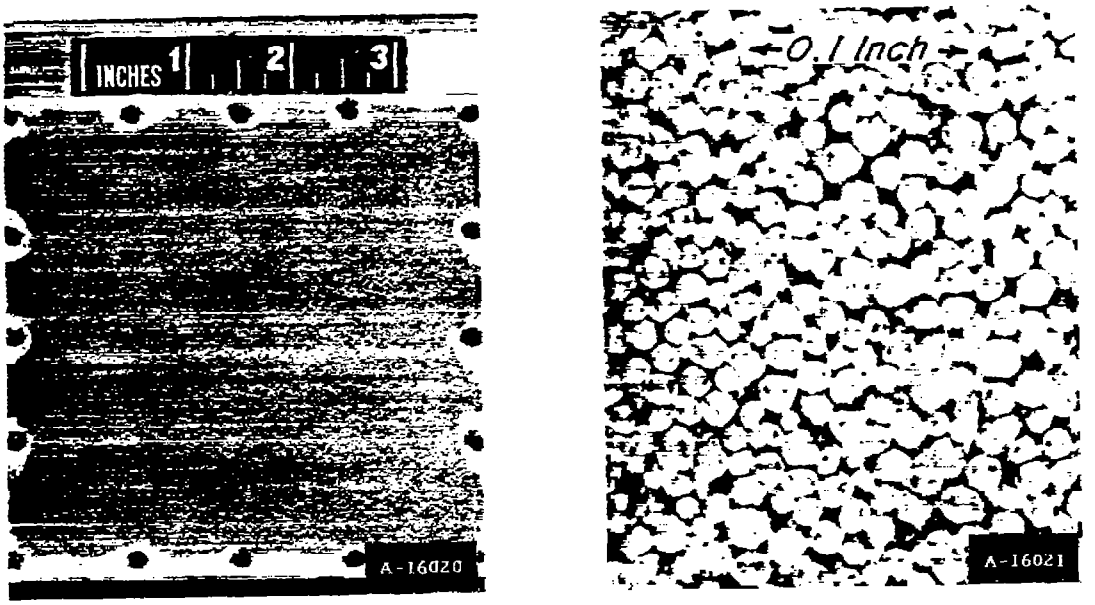

(e) Sample 7 (sintered bronze).

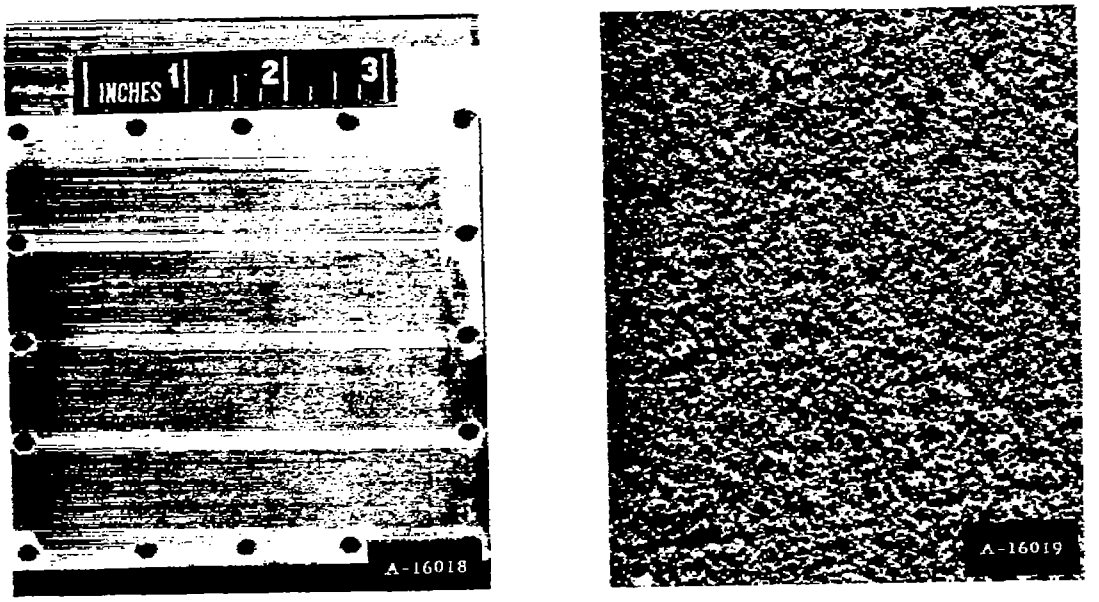

(f) Sample 8 (sintered bronze).

Figure 1.- Continued.

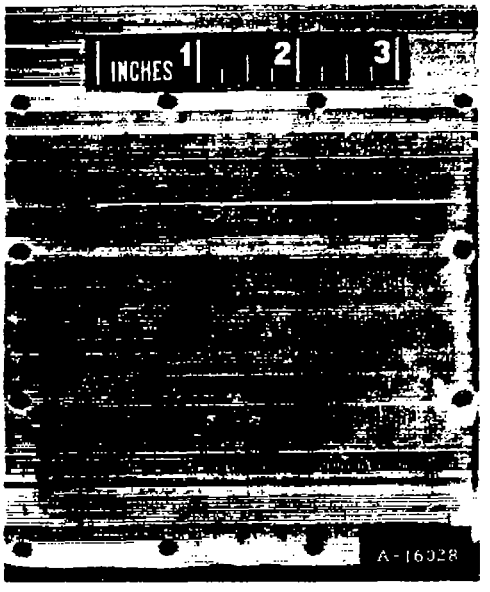

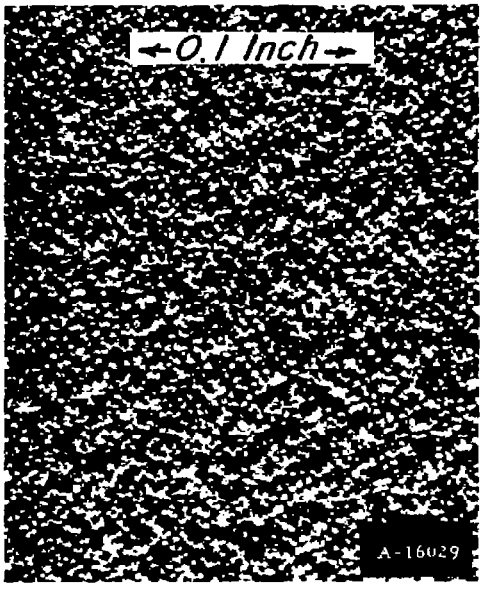

(g) Sample 9 (sintered bronze).

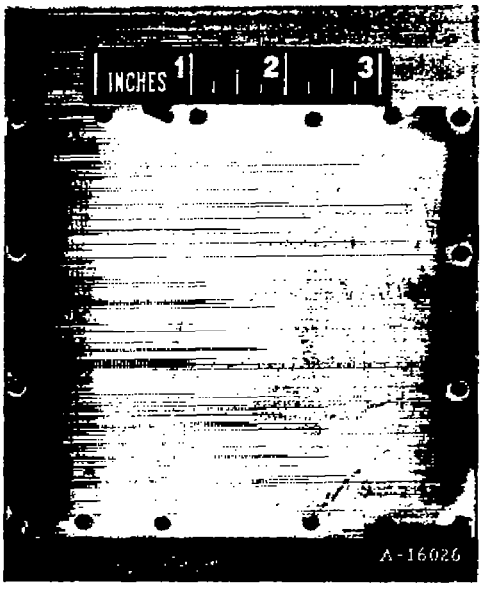

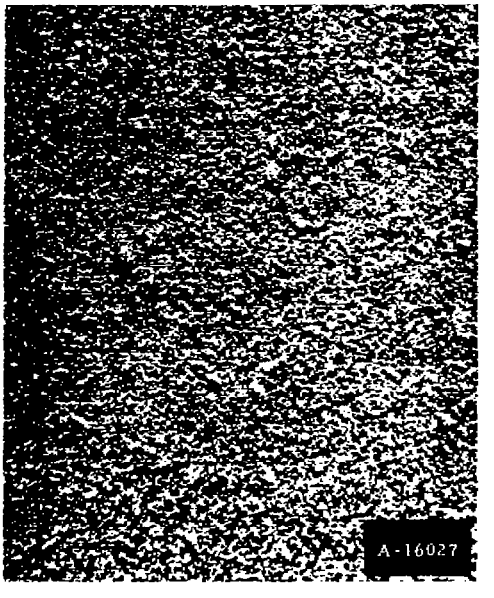

(h) Sample 10 (sintered bronze)

Figure 1.- Concluded.

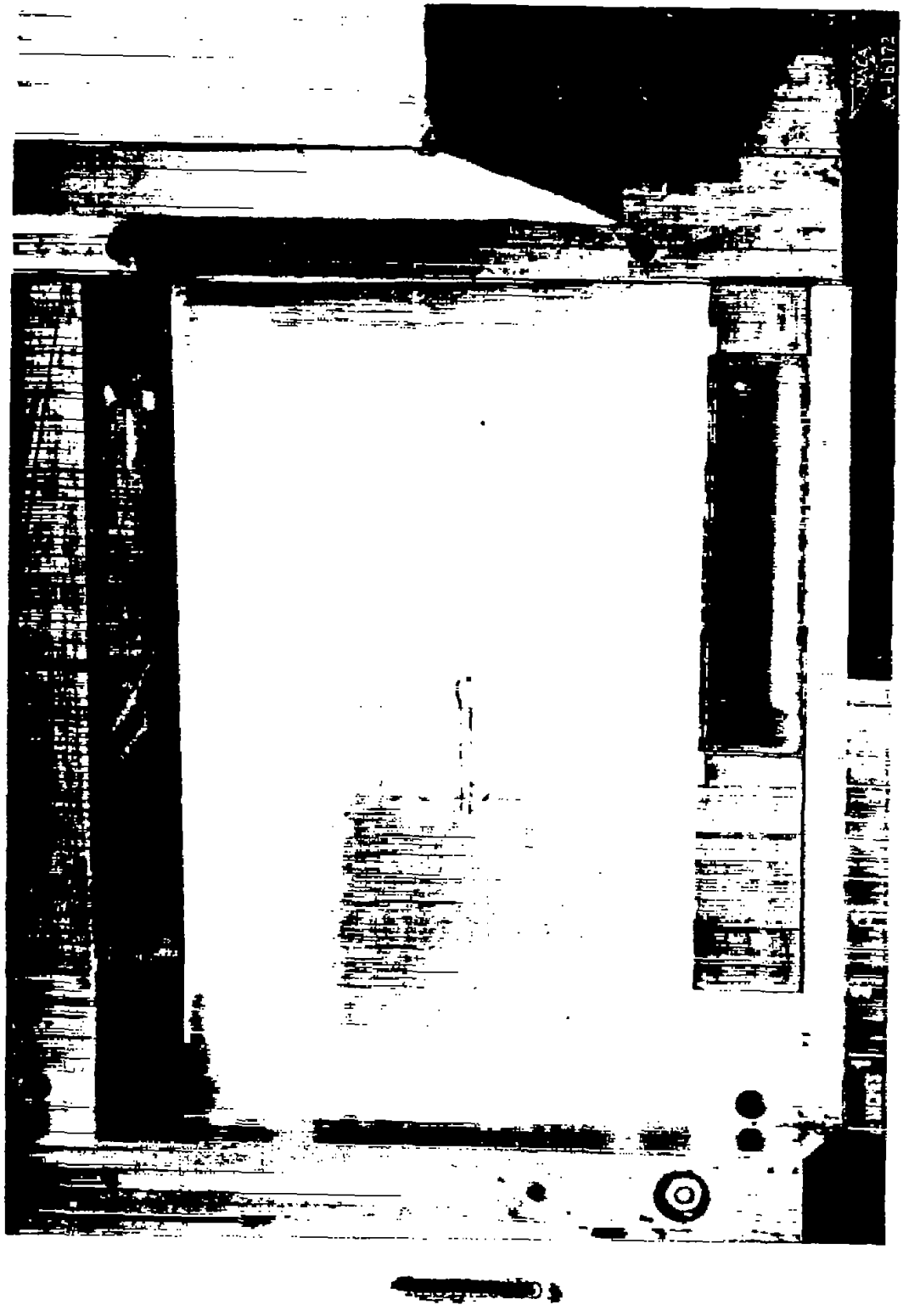

Figure 2.- Test sample mounted in the wind tunnel.

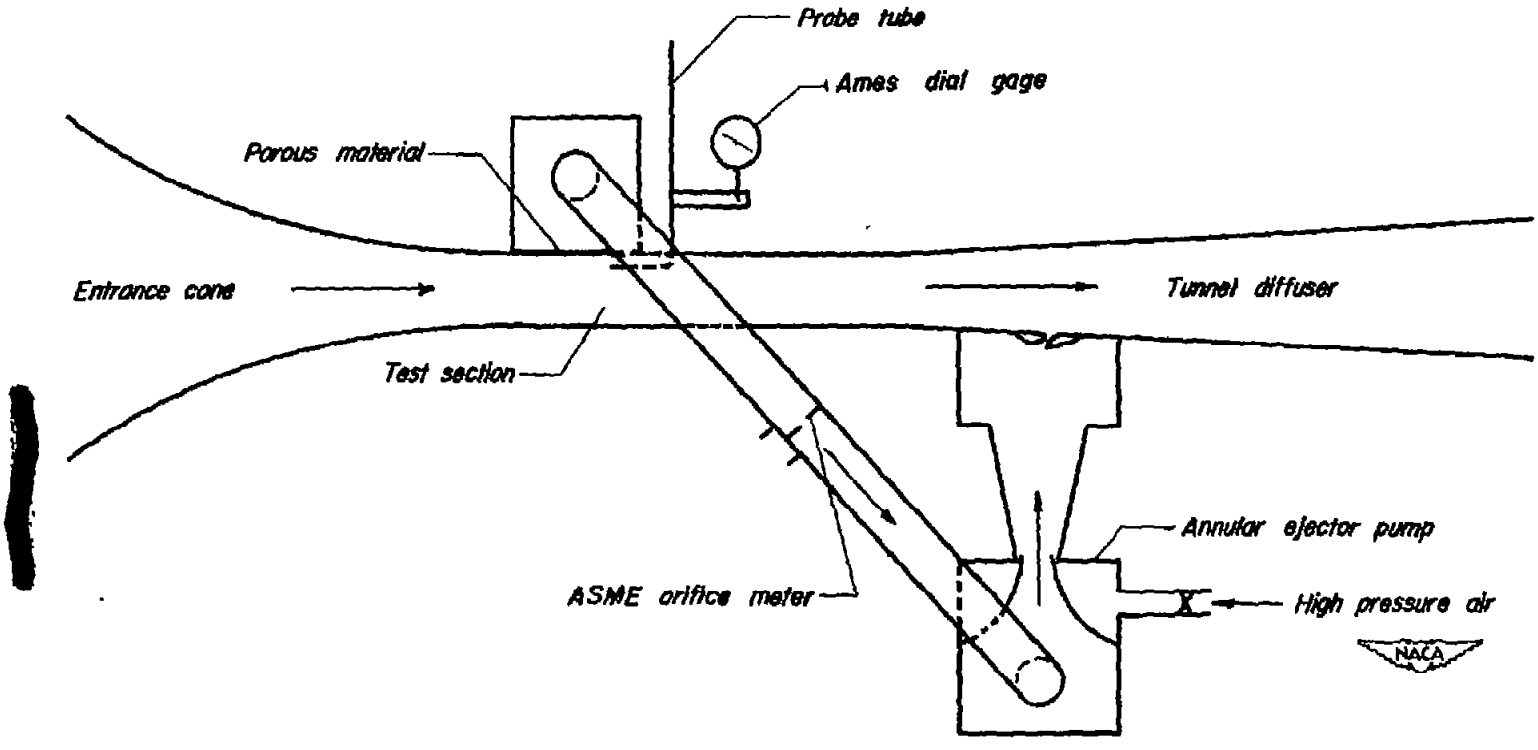

Figure 3.- Diagram of test setup.

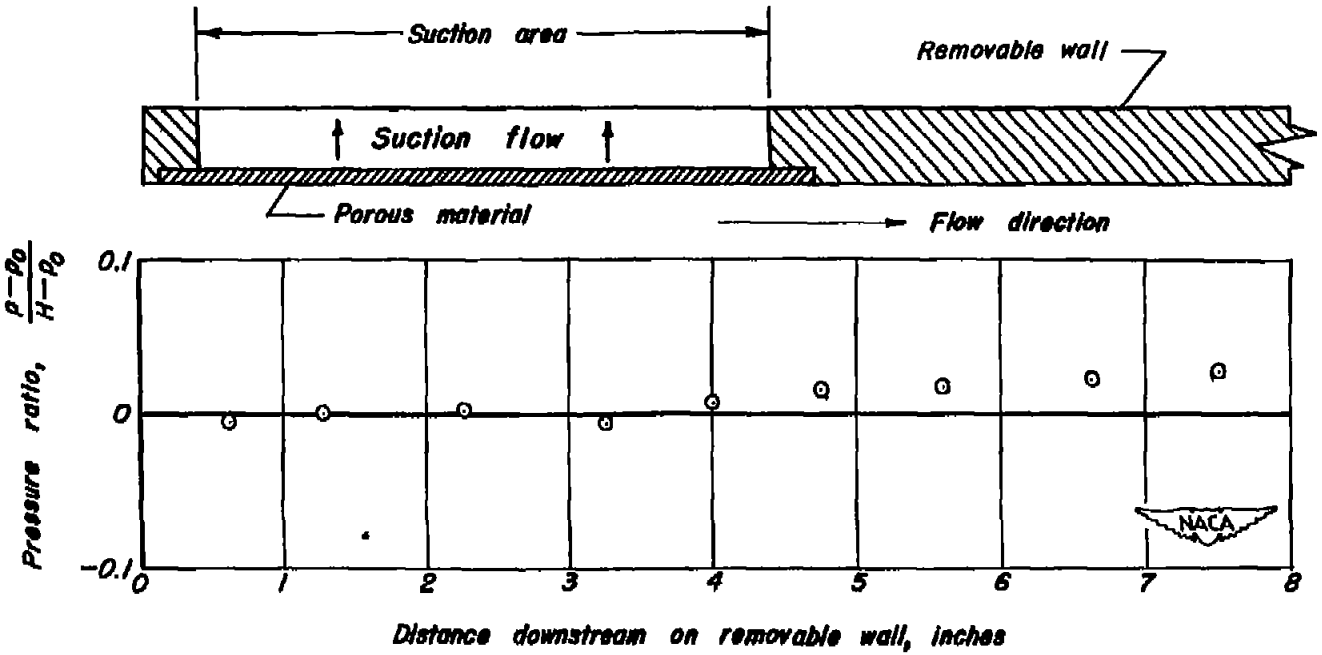

Figure 4.— Pressure distribution along horizontal center line of test-section wall.

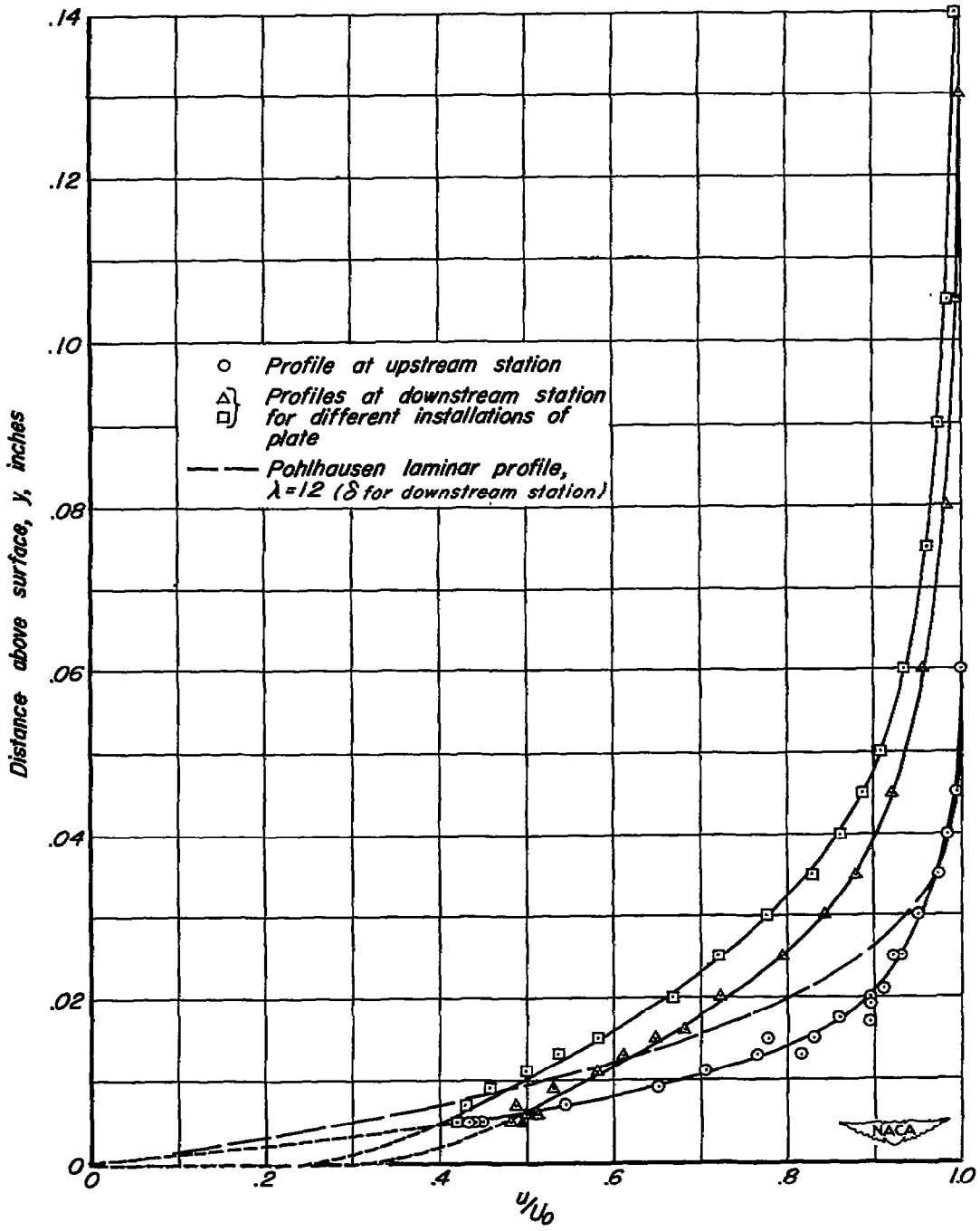

Figure 5.- Boundary-layer velocity profiles on impervious aluminum plate.

[redacted]

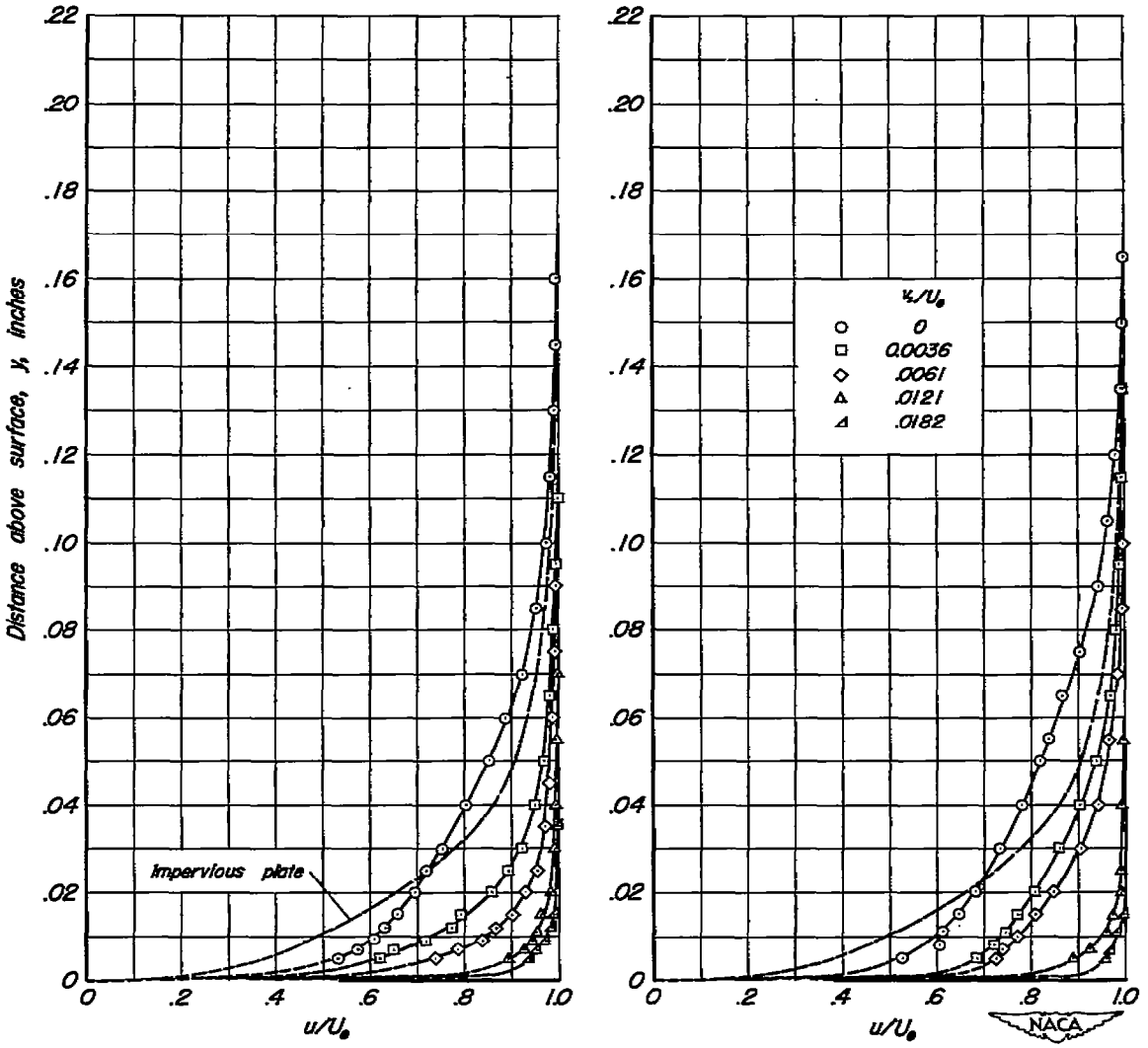

(a) Sample 1, (filter paper with wire screen backing).

(b) Sample 2, (filter paper with electroplated mesh backing).

Figure 6.—Boundary-layer velocity profiles on several porous materials with various suction velocities.

[redacted]

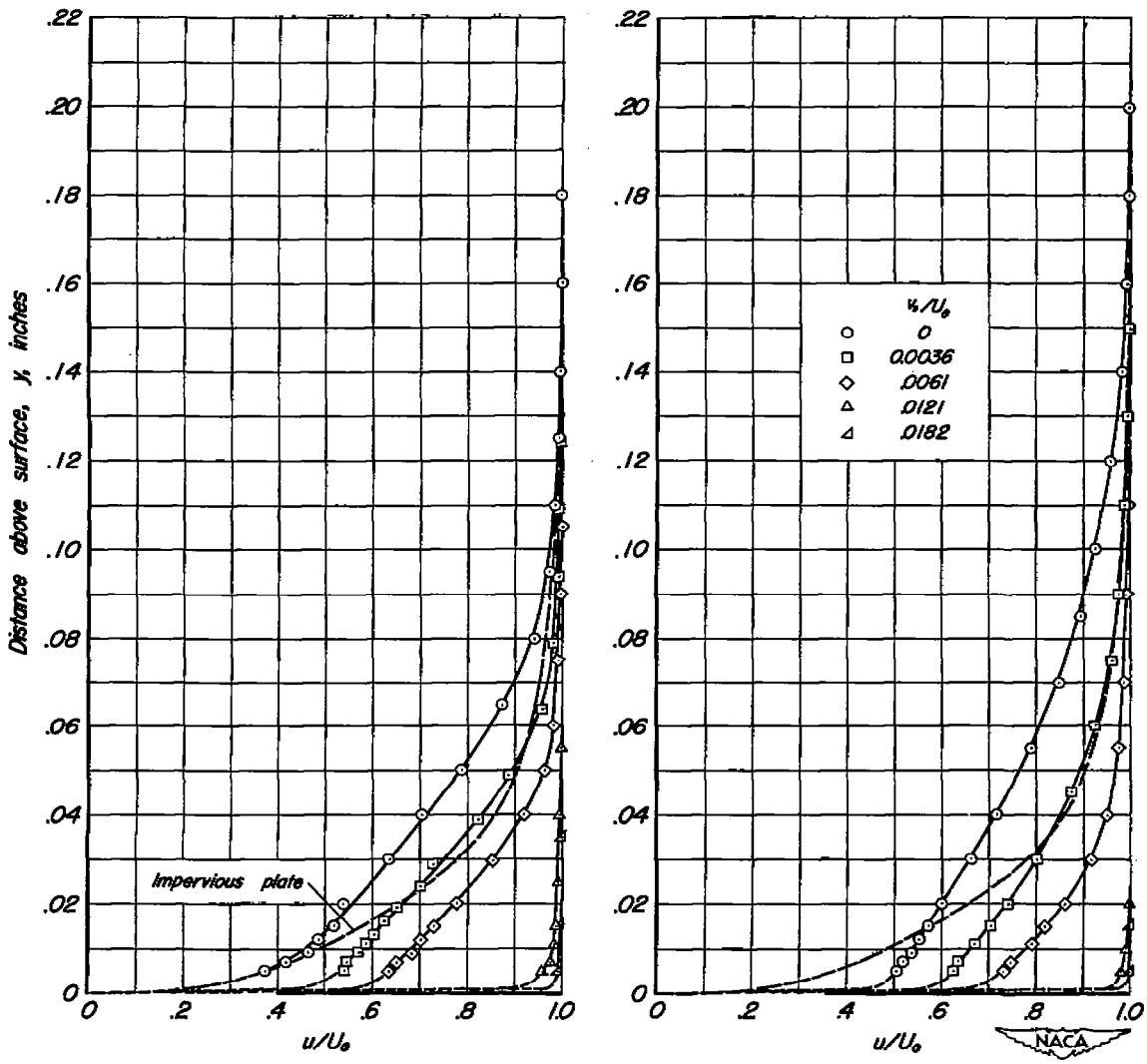

(c) Sample 3, (wire cloth with woof parallel with flow).

(d) Sample 4, (wire cloth with warp parallel with flow).

Figure 6 .—Continued.

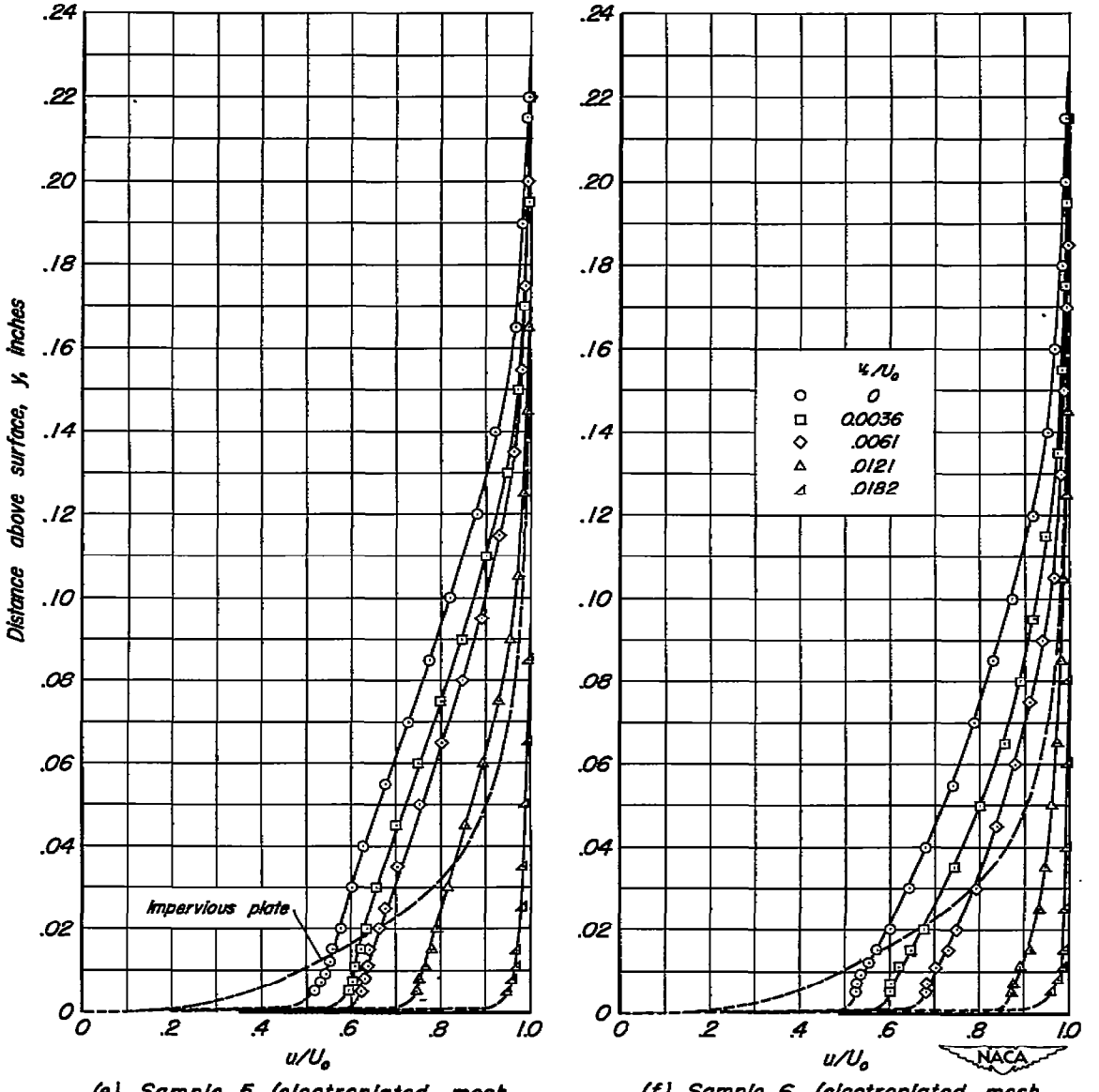

(e) Sample 5, (electroplated mesh, 40 count).

(f) Sample 6, (electroplated mesh, 65 count).

Figure 6.—Continued.

[redacted]

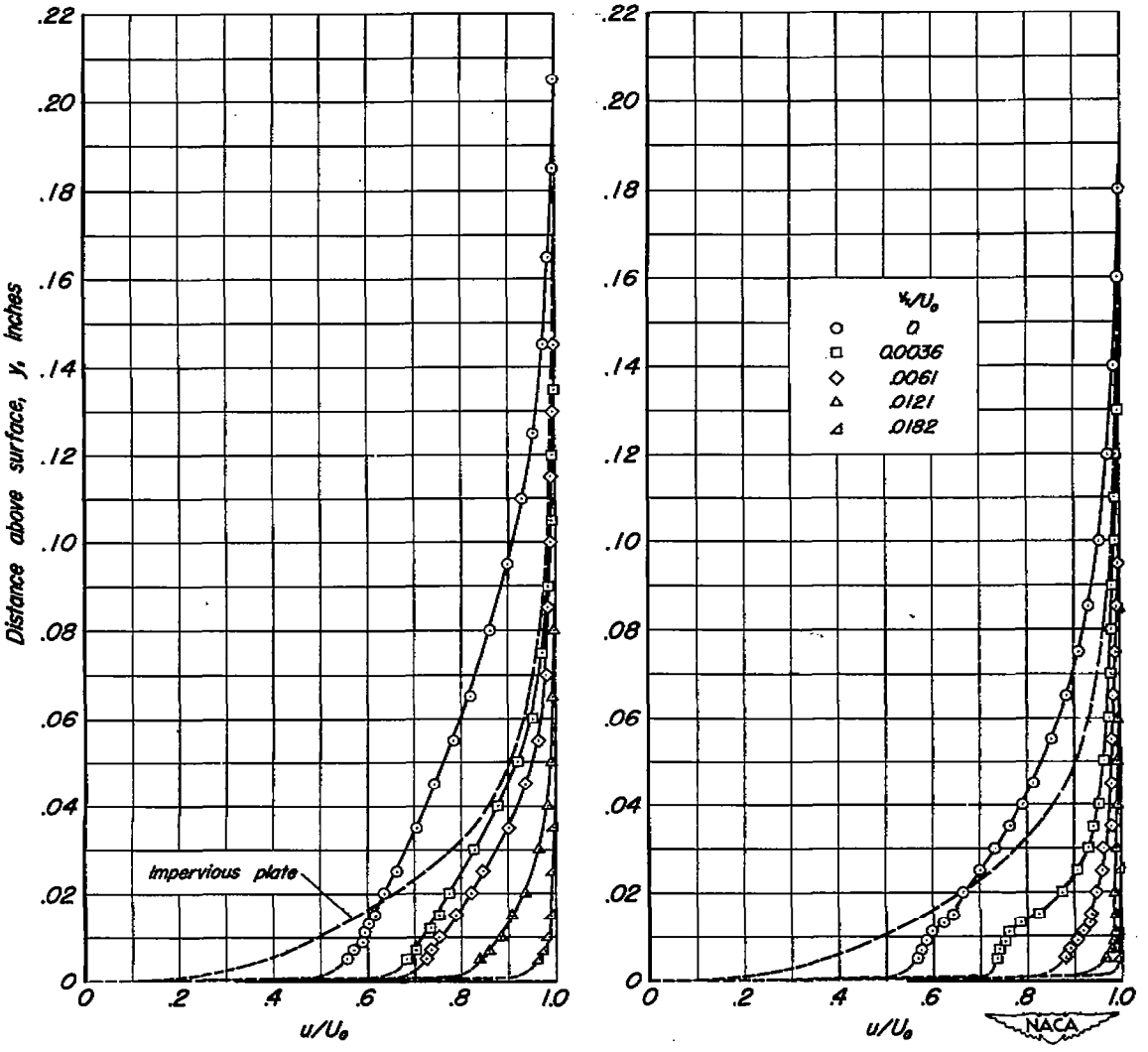

(g) Sample 7, (sintered bronze). (h) Sample 8, (sintered bronze).

Figure 6 .- Continued.

[redacted]

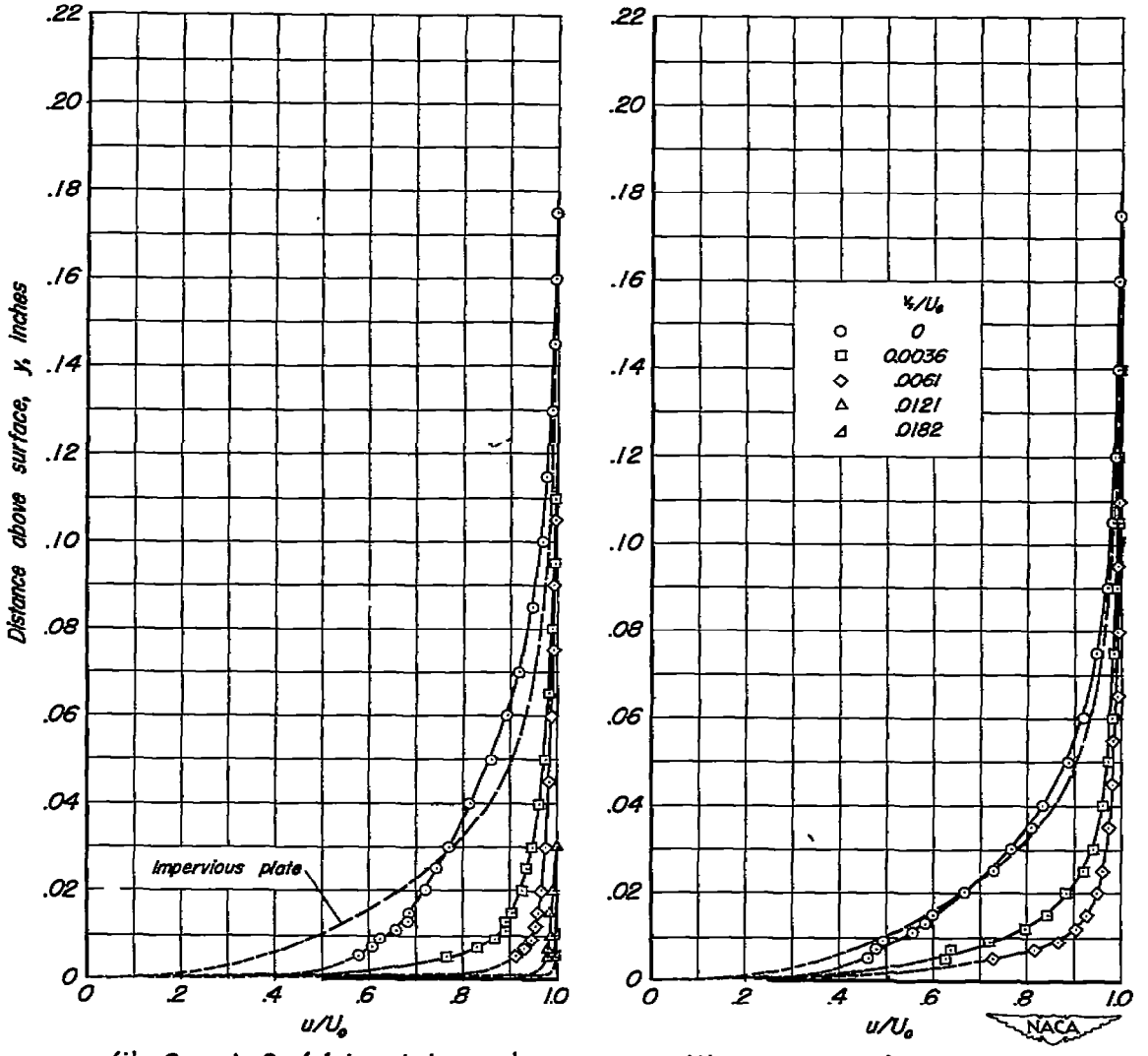

(i) Sample 9, (sintered bronze).

(j) Sample 10, (sintered bronze).

Figure 6 .– Concluded.

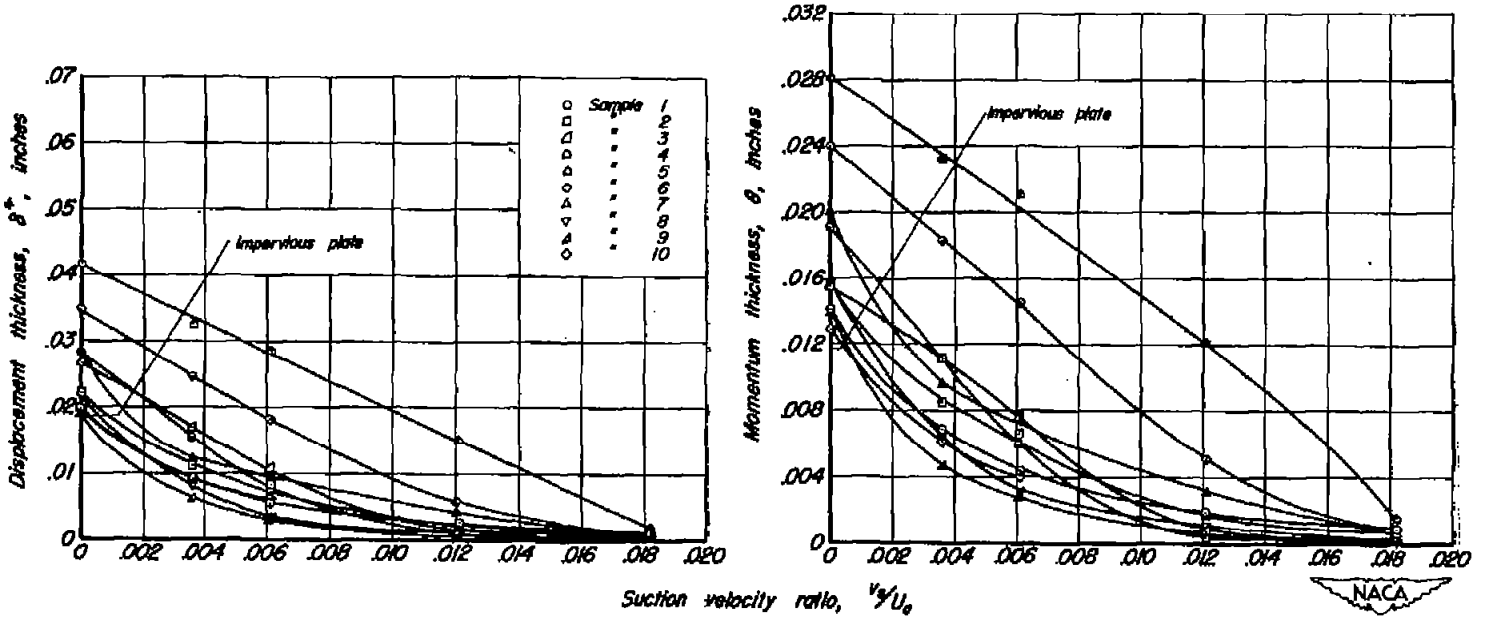

Figure 7.– Variation of boundary-layer displacement thickness and momentum thickness with suction velocity ratio.